Thesis for the degree of Licentiate of Engineering

Holographic descriptions of collective modes in strongly correlated media

Marcus Tornsö

Department of Physics
Chalmers University of Technology
Gothenburg, Sweden, 2019

Holographic descriptions of collective modes in strongly correlated media
Marcus Tornsö

Department of Physics
Chalmers University of Technology
SE–412 96 Gothenburg
Sweden
Telephone +46 (0)31-772 1000

Chalmers Reproservice
Gothenburg, Sweden, 2019

Holographic descriptions of collective modes in strongly correlated media
MARCUS TORNSÖ
Department of Physics
Chalmers University of Technology

Abstract

Solving the puzzle of high temperature superconductivity may be one of the most desired scientific breakthroughs of our time, as access to room temperature superconductivity could revolutionize society as we know it. In this thesis, we strive to increase the theoretical understanding of such matter, by studying the phase above, in temperature, the superconducting phase - the "strange metal".

The strange metal phase is a phase characterized by the absence of a quasi-particle description. The electrons in this phase are strongly coupled, which means that conventional methods, such as perturbation theory in quantum field theory and Monte Carlo methods fall short of being able to describe their dynamics. Perhaps surprisingly, string theory provides a different method, capable of describing precisely such systems - the holographic duality.

Whereas there has been significant effort devoted to the applications of the duality since its inception in 1997, and even more so in the last decade after it was observed that it worked remarkably well for condensed matter theory, it wasn't until our project that the dynamical polarization of such strongly coupled systems where properly treated.

In this thesis, we introduce the minimal constraints required for a sensible description of a polarizing medium, and convert those to boundary conditions to the equations of motion provided by the holographic dual. These boundary conditions deviate from previous holographic studies, and we contrast the quasinormal modes previously studied with the emergent collective modes we find for some different models.

We find novel results, as well as confirm the predictions of less general models in their respective regions of validity and pave the way for more complex future models.

Keywords: holography, plasmonics, strong coupling, graphene, quasinormal modes, gauge/gravity duality, strongly correlated media

Publications

This thesis is based on the following publications:

[I] **Holographic plasmons**
U. Gran, M. Tornsö, T. Zingg
J. High Energ. Phys. (2018) 2018: 176.
https://doi.org/10.1007/JHEP11(2018)176

[II] **Plasmons in holographic graphene**
U. Gran, M. Tornsö, T. Zingg
arXiv:1804.02284.
https://arxiv.org/abs/1804.02284

[III] **Exotic Holographic Dispersion**
U. Gran, M. Tornsö, T. Zingg
J. High Energ. Phys. (2019) 2019: 32.
https://doi.org/10.1007/JHEP02(2019)032

[IV] **Holographic Response of Electron Clouds**
U. Gran, M. Tornsö, T. Zingg
J. High Energ. Phys. (2019) 2019: 19.
https://doi.org/10.1007/JHEP03(2019)019

Other publications by the author that are not included in the thesis:

- **Holographic Plasmon Relaxation with and without Broken Translations**
  M. Baggioli, U. Gran, A. Jimenez Alba, M. Tornsö, T. Zingg
  arXiv:1905.00804
  Accepted for publication in JHEP.
  https://arxiv.org/abs/1905.00804

Contents

Acknowledgments

Firstly, I want to thank my supervisor Ulf Gran, without whom this project would not have been possible. I would also like to thank my assistant supervisors Bengt Nilsson and Henrik Johannesson for their support. I would also like to thank Tobias Wenger and Andreas Isaksson for many insightful discussions. Also, my collaborators Tobias Zingg, Niko Jokela, Alfonso Ramallo Vasquez and Daniele Musso for their intellectual contributions to my knowledge. My thanks to the Division of Theoretical Physics for taking me on, and helping me along the way. Lastly, for their persistent support, I thank my family and my friends.

Marcus Tornsö, 2019

Chapter 1

Introduction

This thesis concerns the topic of describing plasmons, collective modes and quasinormal modes (QNM) in strongly correlated matter using holography. In particular, it covers such modes for two- and three-dimensional systems, with materials such as graphene and cuprates as their respective end goals to describe.

A strong scientific interest in strongly coupled media is warranted by their immense potential, with high-temperature superconductivity being arguably the most important. Conventional superconductivity was discovered as early as 1911 [1], a property observed for certain materials when they are cooled to very low temperatures. A material displaying superconductivity, a superconductor, exhibits no electrical resistivity, and as a direct consequence expels all magnetic fields. There are many important and highly non-trivial consequences from this, among the more famous that magnets can levitate above superconductors stably – as there is no energy required for electrical currents, it produces its own current to essentially act as a repulsive electromagnet, without any external contribution. Lossless transport of both electricity and vehicles are revolutionary applications that immediately come to mind, but it's uses also spans to more technical purposes, such as quantum computing.

The mechanism behind conventional superconductivity was worked out in the 1950s by Bardeen, Cooper and Schrieffer [2], in what is now called BCS-theory, and for which they received the Nobel prize in 1972. The main take away is that electrons in a material can pair up into *Cooper pairs*, which are composite bosons rather than fermions, meaning they can all occupy the same quantum state, giving rise to the degenerate ground state that provides superconductivity. However, these composite pairs are frail, and can thus only exist at very small temperatures before they thermally dissolve. With that result, it seemed highly unlikely that superconductivity would ever reach outside cryogenics laboratories. But, in 1986, Bednorz and Müller discovered the existence of high-temperature superconductors [3]

and were subsequently awarded the Nobel prize the following year. To date, compounds have been found that are superconducting to temperatures even above 100K. Whereas this may still seem far away from room temperature ($\sim$ 300K), it is worth pointing out that it is still on same order of magnitude, and our understanding of these unconventional superconductors is still very limited (and given the history of superconductors, a Nobel prize is up for grabs).

These superconductors are thus very enticing to study, but lack a proper theoretical description. To better understand the critical temperature, the point at which a compound becomes superconducting, we need better understanding of the phase on the other side of it, the so-called "strange metal". This aptly named phase is characterized by the absence of long-lived quasiparticles, and is governed by strong coulomb interactions, without simultaneously being described as a Fermi-liquid – which is what makes ordinary metals, although strongly coupled, possible to be described as well as they already have been. This absence eliminates the possibility of using conventional tools such as perturbation theory or Monte-Carlo methods to describe strange metals and thus there is a need for other, alternative methods to model them. Holography is one of very few promising candidates to approach these materials, as the holographic duality allows for a weakly coupled dual description of the underlying strongly coupled QFT.

Strange metals being an uncharted territory of physics is of course by itself another reason to conduct this type of research.

Similarly, there has been an explosive interest in graphene, since it's discovery in 2004, and subsequent Nobel prize in 2010. Graphene, being as perfectly two-dimensional as allowed by nature, has many very extreme general properties, such as it's strength, electrical and thermal conductivity, optical transparency and many more specific, such as e.g. its electrons behaving as essentially massless particles. This has led to many ambitious research projects, e.g. the EU's Graphene Flagship project. If that wasn't enough, graphene also has a strange metal phase. Near its charge neutrality point, graphene exhibits strong coupling, indicating that more exotic properties could be obtained. Although predicted theoretically, this phase is difficult to model more exactly. Once again, this motivates holographic studies, but this time for a very different type of material.

There are many different properties of strange metals one could possibly want to describe, and many of them are accessible to holographic methods. In this thesis, motivated by the fundamentally interesting properties behind superconductors being how charge carriers interact, we have chosen to focus on the charge response of holographic models. In particular, we have looked at the modes of such systems. There are fundamentally two kinds of modes; quasinormal modes, which correspond to poles in the screened response function χ_{sc} or alternatively to driven excitations, and collective modes, which corresponds to poles in the full dynamic response function

χ or equivalently to self-sourced modes. The most easily excited collective mode, is what we refer to as the "plasmon" mode. Conventional plasmons are ubiquitous in conducting media, and are quanta of plasma oscillations (plasma here referring to the free electrons in the metal). For a system without a quasiparticle description, such a definition is of little use, but they are fundamentally related by the previous definition, as the lowest, propagating and self-sourced excitation of a plasma. Motivating the study of the other type of mode, the quasinormal mode, may from the perspective of a strange metal be difficult, but on the other side of the holographic duality, such excitations corresponds to the most fundamental excitations, and collective excitations are much more contrived, which is likely the reason why we were among the first to study them.

Plasmons themselves have many interesting properties, and their close relation to both electrical currents and light often make them the ideal choice when it comes to miniaturization of circuits [4, 5] or making hyperfast and sensitive detectors [6]. The usage of plasmons in technology is a scientific field in its own right, *plasmonics*. Many applications of plasmons relate to a strong wave localization of plasmons compared to light. Graphene exhibits a very strong such localization [7], making it an ideal candidate for many plasmonic applications. There thus exist good reasons to examine strongly coupled plasmonics, both for two- and three-dimensional materials, which is what our research has been focused on.

This thesis is structured as follows. In chapter 2, an introduction to plasmons (and other types of electromagnetic modes) from Maxwell theory is given, as well as the predictions from a few common models at weak coupling. Chapter 3 gives a brief introduction to strange metals, the quantum matter that is the target for this thesis. In chapter 4, the holographic duality is presented and the method in which it can be adapted for condensed matter studies, in particular which is done in papers I-IV. From the studies in these papers, some future directions for research is outlined in chapter 5. Lastly, short summaries of papers I-IV is given in 6, as a description of my personal contributions to these works.

Chapter 2

Plasmons

Plasmons are per definition excitations of a plasma. A plasma is much like a gas, but rather than having a composition of neutral atoms or molecules, a plasma is made of charged ions. As such the forces between individual particles are much stronger than compared to ordinary gasses. Plasma is often considered the fourth phase of matter, after solid, liquid and gas, and it is typically in that order they transition into each other with increasing temperature or, correspondingly, decreasing pressure.

However, this is not the type of plasma we primarily aim to describe here. We instead consider metals, i.e. solids, but where a rigid crystalline lattice of positively charged nuclei is filled with more or less bound negatively charged electrons. If the electrons are not all bound by the nuclei, then one can consider the metal as a background of positively charged ions, in which a density of electrons is free to move, very much like a plasma. The movement of the electrons is typically slow, and as they interact with strong Coulomb forces, their behaviour is more like that of a liquid. Certain properties can be well described by traditional hydrodynamic methods. It is therefore not uncommon that the electron plasma, inside a solid, is referred to as a gas or a liquid as well. The nomenclature is far from perfect.

Plasmons are quanta of wavelike excitations in this plasma, much like sound waves. However, compared to sound waves they have a more complicated frequency dependence, with several qualitatively different effects, such as e.g. highly frequency dependent velocities.

The most fundamental plasma excitation is typically only referred to as plasma oscillation. Here, the plasma simply oscillates back and forth without propagating, at a fixed frequency determined by the system, the so-called plasma frequency, ω_p. This can actually be derived rather straightforwardly, one way is shown in section 2.3.1. These excitations can also propagate if one introduces a wavelength and they are also commonly referred to as Langmuir waves.

There are multiple types of plasmons. One way to separate them is

whether the charged particles move in the same direction as the wave (longitudinal) or in a perpendicular direction (transversal). There are also localized plasmons (confined to nanoparticles). There is also a distinction between bulk and surface plasmons. Bulk plasmons can roughly be categorized as living in a medium that is homogeneous (or even isotropic) - i.e. there is no significant difference in different points. Surface plasmons do not fulfill that criteria. A surface plasmon lives on the interface between two media (e.g. the surface on a metal, the plasmon has metal on one side, air on the other). These are also sometimes known as polaritons (implying they are a hybridization of a charge wave in the medium and a field wave outside). It should also be mentioned that arguably surface plasmons could be separated into two categories itself, interface plasmons – where the plasmons essentially live on the boundary of a material, with another medium next to it, and sheet or 2D plasmons – where the plasmons effectively live in a thin sheet, with different media on both sides. In the literature, the latter is often discussed in the context of 2D electron gasses (2DEG), but some sheets, e.g. graphene, have extreme properties that often exclude them from that category. Specifically, graphene can have a strong coupling and the free electrons are then better described as a fluid than a gas. This is often referred to as the Dirac fluid phase.

In this thesis, we focus mainly on longitudinal bulk and 2D plasmons.

2.1 History

Where plasmons are relatively difficult to describe, and were first so in the 20th century, they have unknowingly been used for centuries, back to as early as 400 AD. Phenomenologically, surface plasmons are easily excited by incident light on smooth metallic surfaces where they live for a short while, before they decay, and re-emit the light. Some wavelengths are more difficult to absorb than others, which means there will be a coloring effect. This effect has for instance been used by the Romans to dye cups and later by adding small metallic beads to stain glass windows to different colors [8, 9]. As the plasmons move along the surface of the metallic beads and re-emit the light in a different direction, this method of colouring glass has the neat effect that transmitted and reflected light has different colours, meaning the colours change depending on the position of the light source relative to the viewer.

The underlying physics was of course unknown then. Not until Maxwell compiled his famous equations in 1861 were plasmons even possible to describe, and it wasn't until the 1920s they were "discovered" by Langmuir and Tonks [10]. In 1956 they were properly described in their quantized form by Pines[11].

Today, plasmons are used extensively, enough so for "plasmonics" to

be a proper field in itself [12, 13]. They are used in spectroscopy for signal enhancing (e.g. surface enhanced Raman spectroscopy, SERS) and in extremely sensitive detection of nanoparticles (e.g. detection of flammable gasses in cars and factories).

A lot of the interest in plasmons comes from the large wave localization they bring, allowing for the miniaturization of circuits and also localization of energy, which brings the great enhancement in SERS.

2.2 Properties

Plasmons can be well described with classical electromagnetism, where the interaction between charged particles is governed by Maxwell's equations,

$$\nabla \cdot \boldsymbol{E} = \frac{\rho}{\epsilon_0}\,, \tag{2.1}$$

$$\nabla \times \boldsymbol{B} - \frac{1}{c^2}\frac{\partial \boldsymbol{E}}{\partial t} = \mu_0 \boldsymbol{J}\,, \tag{2.2}$$

$$\nabla \cdot \boldsymbol{B} = 0\,, \tag{2.3}$$

$$\nabla \times \boldsymbol{E} + \frac{\partial \boldsymbol{B}}{\partial t} = 0\,. \tag{2.4}$$

Here $\boldsymbol{E}$ is the electric field, $\boldsymbol{B}$ is the magnetic field, ρ is the charge density and $\boldsymbol{J}$ is the current density. ϵ_0 and μ_0 are the permittivity and permeability of vacuum respectively. These equations were found individually, and as such have individual names with which they are sometimes referred to as: (2.1) is Gauss' law, (2.2) is Ampère's law, (2.3) is Gauss' law for for magnetism and (2.4) is Faraday's law. From these many familiar relations can be derived, most notably the continuity equation,

$$0 = \nabla \cdot \boldsymbol{J} + \frac{\partial \rho}{\partial t}\,, \tag{2.5}$$

equating the flow of charges to the change in charge density at any point, and thus the charge of a system is preserved.

It is often convenient to separate the macroscopic contributions from the response of a medium and the applied fields from the total fields $\boldsymbol{E}$ and $\boldsymbol{M}$. We introduce the polarization $\boldsymbol{P}$ of the medium as the response of an applied displacement field $\boldsymbol{D}$, the magnetization $\boldsymbol{M}$ of the medium as the response to an applied magnetizing field $\boldsymbol{H}$. It should be mentioned that this viewpoint is generally useful, although there are situations where the polarization and magnetization are not the response to external fields, e.g. electrets and ferromagnets. We also separate the different contributions to the densities, into an induced charge density $\langle\rho\rangle$, an induced current density $\langle\boldsymbol{J}\rangle$, an applied external charge ρ_{ext} and an applied external current

$\boldsymbol{J}_{ext}$. Specifically, these are

$$\boldsymbol{E} = \frac{1}{\epsilon_0}\left(\boldsymbol{D} - \boldsymbol{P}\right), \tag{2.6}$$

$$\boldsymbol{B} = \mu_0\left(\boldsymbol{H} + \boldsymbol{M}\right), \tag{2.7}$$

$$\rho = \rho_{ext} + \langle\rho\rangle, \tag{2.8}$$

$$\boldsymbol{J} = \boldsymbol{J}_{ext} + \langle\boldsymbol{J}\rangle. \tag{2.9}$$

Where the induced charge and current densities are often difficult to keep track of as that would require a proper microscopic description of the materials. The external ones are however very natural, allowing us to write Maxwell's equations in a convenient macroscopic way, turning (2.1) and (2.2) into

$$\nabla \cdot \boldsymbol{D} = \rho_{ext}, \tag{2.10}$$

$$\nabla \times \boldsymbol{H} - \frac{\partial \boldsymbol{D}}{\partial t} = \boldsymbol{J}_{ext}. \tag{2.11}$$

Similarly, one can formulate continuity equations for induced and external charges and currents as well.

Furthermore, by defining the dielectric function, ϵ, by

$$\boldsymbol{D} = \epsilon\boldsymbol{E}, \tag{2.12}$$

the conductivity, σ, by

$$\langle\boldsymbol{J}\rangle = \sigma\boldsymbol{E}, \tag{2.13}$$

one can write the solutions of these equations in a more explicit manner. Note that the quantities ϵ and σ in general are matrices. These matrices account for measurable and important quantities of any medium, furthermore they are linked to each other by the equations above. They can also depend non-trivially on the field strength $\boldsymbol{E}$ itself, effectively making the material inhomogeneous and time-dependent for varying fields. However, in general, a system can be treated in linear response, assuming small fields and thus negligible higher order contributions to σ and ϵ.

With these definitions, one can extract a relation between σ and ϵ. Differentiating the difference between (2.10) and (2.1) with respect to time, substituting $\boldsymbol{D}$ as in (2.12) and ρ using the continuity equation and $\boldsymbol{J}$ as in 2.9 and (2.13), one finds

$$\frac{d}{dt}\left[\nabla \cdot \left(\epsilon_0 - \epsilon\right)\boldsymbol{E}\right] = -\nabla \cdot \sigma\boldsymbol{E}. \tag{2.14}$$

In linear response it becomes natural to assume the medium to be homogeneous (unchanging in space) and time-independent. A common situation is also to study isotropic media, in which the dielectric function and conductivity are the same in all directions. The derivatives then commute with σ and ϵ and we can simply move them to the fields,

$$\left[(\epsilon_0 - \epsilon)\,\frac{d}{dt} + \sigma\right] \nabla \cdot \boldsymbol{E} = 0\,. \tag{2.15}$$

That is, when $\nabla \cdot \boldsymbol{E} \neq 0$, which is the case for longitudinal modes, the expression in brackets has to be zero. For individual frequencies, i.e. the time dependence of $\boldsymbol{E}$ is proportional to $e^{-i\omega t}$, this means

$$\epsilon = \epsilon_0 + i\frac{\sigma}{\omega}\,. \tag{2.16}$$

It is worth pointing out here that defining the electric susceptibility χ_P as

$$\boldsymbol{P} = \chi_P \boldsymbol{E}\,, \tag{2.17}$$

(2.16) simply yields

$$\chi_P = i\frac{\sigma}{\omega}\,. \tag{2.18}$$

2.2.1 The plasmon condition

As previously stated, there are multiple types of excitations of a system. The importance of external charges of currents is manifest in equations (2.10)-(2.11). The excitations we refer to as plasmons are self-sourced excitations, i.e. they are solutions to Maxwell's equations in the absence of external influence. Equation (2.10) then implies that

$$\epsilon = 0\,, \tag{2.19}$$

which is what we refer to as the *plasmon condition*, or that the solution is trivial, i.e. $\boldsymbol{E} = \langle \boldsymbol{J} \rangle = 0$.

It is worth mentioning that plasmons commonly refer to a specific subset of the solutions to this condition that are propagating, or even only the lowest energy solution of these. In fact, since the absence of external charges is something that is common for collective excitations, we refer to the solutions as collective modes, however, in general it's the lowest propagating collective mode that is of interest, i.e. the plasmon mode.

Another common type of mode to describe are quasinormal modes (QNM). These are poles of the conductivity, or the screened density-density correlator

$$\chi_{sc} = \langle \rho\, \rho \rangle = \frac{k^2}{i\omega}\sigma\,, \tag{2.20}$$

whereas collective modes are the poles of the full density-density correlator [14],

$$\chi = \chi_{sc}/\epsilon\,. \tag{2.21}$$

QNMs correspond to solutions where you can have an induced current, even without an electric field, with a driving external current. They are interesting in their own right, and are closely related to collective modes.

2.2.2 In terms of potentials

The governing equations are commonly solved in terms of electromagnetic vector potentials, i.e.

$$\boldsymbol{E} = -\frac{\partial \boldsymbol{A}}{\partial t} - \nabla\phi\,. \tag{2.22}$$

Looking at equation (2.2) in the absence of a magnetic field we find

$$-\epsilon_0 \dot{\boldsymbol{E}} = \langle \boldsymbol{J} \rangle\,. \tag{2.23}$$

Without loss of generality, choosing the momentum to be in the x-direction and choosing $\phi = 0$ gauge, this equation can be written as

$$\omega^2 A_x + J_x = 0\,. \tag{2.24}$$

Similarly, in Coulomb gauge (with $\boldsymbol{A} = 0$), it can be written

$$k^2\phi - \rho = 0\,. \tag{2.25}$$

For quasinormal modes, $\boldsymbol{J} = 0$ and thus the condition simply becomes

$$\phi = 0\,, \qquad A_x = 0\,. \tag{2.26}$$

2.2.3 Codimension

The fundamental difference between studying bulk plasmons and 2D plasmons, is that for the latter, the charges are confined to to a sheet of one less dimension. The mathematical term for this system is that it's a codimension 1 system. It can be shown that for plasmons, the codimension is a very important quantity, more so than the number of dimensions of the system itself. One straightforward way to show this is to compute the contributions from the Coulomb potential[1] of a system,

$$\delta\phi(t, \boldsymbol{r}) \;=\; \int \mathrm{d}^3 r' \frac{\delta\rho(t, \boldsymbol{r}')}{4\pi|\boldsymbol{r} - \boldsymbol{r}'|}\,. \tag{2.27}$$

Keeping the system homogeneous in all three dimensions, returns the previous result of (2.25). However, confining the charges to a plane by factoring in a delta function in one direction yields a different result,

$$k^2\phi - \frac{|k|}{2}\rho = 0\,, \tag{2.28}$$

in Coulomb gauge, and after switching to $\phi = 0$ gauge,

$$\omega^2 A_x + \frac{|k|}{2} J_x = 0\,. \tag{2.29}$$

[1] The concerned reader may worry about the instantaneous-looking Coulomb potential, but will find that it indeed still preserves causality, see e.g. [15].

2.3 Dispersion relations

Equations such as (2.19) are generic for any Maxwell theory, but say very little about the response of any given material. To make a prediction, one needs to further model the compound in some fashion. Where this thesis aims to target strongly coupled materials for which no standard condensed matter theory models are properly available, it is instructive to first consider weakly coupled matter and the already existing models for such.

2.3.1 The Drude Model

The most famous one is probably the Drude model of electrical conduction, which considers collisions of electrons moving in a positively charged lattice with a mean free time of τ, without accounting for any long-range interaction between electrons and lattice or other electrons.

The dynamics are described as

$$\langle \mathbf{p}(t+dt)\rangle = \left(1-\frac{dt}{\tau}\right)\left(\langle \mathbf{p}\rangle + \mathbf{F}dt\right) , \tag{2.30}$$

that is, the time evolution of the momentum is given by the fraction that does not collide times their aggregated momentum due to some force $\mathbf{F}$. To first order in dt, this simplifies to

$$\frac{\partial \mathbf{p}}{\partial t} = -\frac{\mathbf{p}}{\tau} + \mathbf{F} . \tag{2.31}$$

In our case, we can relate the momentum to the current by

$$\mathbf{j} = -\frac{ne}{m}\mathbf{p} , \tag{2.32}$$

where e and m are the charge and mass of the electron, and n is the number density.

For an AC electric field, the force is given by

$$\mathbf{F} = -e\mathbf{E}(t) = -e\mathbf{E}\, e^{-i\omega t} , \tag{2.33}$$

and the momentum can be assumed to take the same form, $\mathbf{p}(t) = \mathbf{p}\, e^{-i\omega t}$, which yields a conductivity

$$\sigma(\omega, \boldsymbol{k}) = \frac{ne^2}{m}\frac{\tau}{1-i\omega\tau} . \tag{2.34}$$

This, inserted in (2.16) and (2.19), yields

$$\omega = \frac{-i \pm \sqrt{-1+4\tau^2\omega_p^2}}{2\tau} = \pm\,\omega_p - \frac{i}{2\tau} + \mathcal{O}(\tau^{-2}) , \tag{2.35}$$

where we have defined the plasma frequency,

$$\omega_p = \sqrt{\frac{ne^2}{m\epsilon_0}}\,. \tag{2.36}$$

For a propagating wave, $\mathbf{E}(t,\boldsymbol{x}) = \mathbf{E}\,e^{-i\omega t + i\boldsymbol{k}\cdot\boldsymbol{x}}$, the momentum will once again mirror the form, $\mathbf{p}(t,\boldsymbol{x}) = \mathbf{p}\,e^{-i\omega t + i\boldsymbol{k}\cdot\boldsymbol{x}}$, but as the current picks up a spatial dependence, so does the number density, significantly complicating the derivation. This means that there will locally be density variations, which in turn gives pressure variations that will affect the dynamics as well.

2.3.2 Navier-Stokes

One way of modelling the behaviour of a propagating wave is using linearized Navier-Stokes equations,

$$\frac{\partial \mathbf{j}(\mathbf{r},t)}{\partial t} = -\frac{\mathbf{j}}{\tau} + \frac{n_0 e^2}{m}\mathbf{E}(\mathbf{r},t) - \beta^2 e \nabla \delta n(\mathbf{r},t)\,, \tag{2.37}$$

where β is a temperature dependent coefficient.For an ideal gas,

$$\beta^2 = \frac{\gamma k_B T}{m}. \tag{2.38}$$

Using the continuity equation

$$e\frac{\partial \delta n}{\partial t} + \nabla \cdot \mathbf{j} = 0\,, \tag{2.39}$$

and considering individual frequencies and wavenumbers (ω and k) by imposing $\mathbf{E}(t,\boldsymbol{x}) = \mathbf{E}\,e^{-i\omega t + i\boldsymbol{k}\cdot\boldsymbol{x}}$, and $\mathbf{j}(t,\boldsymbol{x}) = \mathbf{j}\,e^{-i\omega t + i\boldsymbol{k}\cdot\boldsymbol{x}}$ one arrives at

$$\sigma = \frac{n_0 e^2}{m}\frac{i\omega}{\omega^2 - \beta^2 k^2 + i\omega/\tau}\,. \tag{2.40}$$

Inserting this conductivity in (2.16) and (2.19) gives the dispersion relation

$$\omega = \pm\sqrt{\omega_p^2 + \beta^2 k^2} - \frac{i}{2\tau} + \mathcal{O}(\tau^{-2})\,, \tag{2.41}$$

with ω_p defined as in (2.36). An important thing to note here is that the scale β introduced by the Navier-Stokes equation is not directly dependent on τ, but are in simpler systems (e.g. an ideal gas or fluid) proportional to the temperature T.

Similarly, inserting (2.40) into (2.29) yields

$$\omega = \pm\sqrt{\left(\beta^2 k + \omega_p^2/2\right)\sqrt{k}} - \frac{i}{2\tau} + \mathcal{O}(\tau^{-2})\,, \tag{2.42}$$

which is interesting for two particular reasons. First of all, for small k (and large τ), it goes as

$$\omega \propto \sqrt{k}\,, \tag{2.43}$$

which is a famous result for 2D materials. Furthermore, the damping term becomes increasingly important for small k. An expansion in small k instead reveals two purely imaginary, i.e. non-propagating modes

$$\begin{cases} \omega = -\dfrac{1}{2} i\tau\omega_p^2 k + \mathcal{O}(k^2)\,, \\ \omega = -\dfrac{i}{\tau} + \dfrac{1}{2} i\tau\omega_p^2 k + \mathcal{O}(k^2)\,. \end{cases} \tag{2.44}$$

2.3.3 Other models

Plasmon dispersions can be studied theoretically in various different ways in different number of dimensions, see e.g. [16] for some other weakly interacting examples, both treated classically and with QFT methods. As mentioned above, it is not necessarily that the charges are free to move in a three-dimensional bulk, or that they are confined to a two-dimensional plane that is of importance for the characteristics of the modes above, but that they are confined to move in the same number of, respectively one less dimension than the electromagnetic fields. This means that we would expect essentially the same behaviour if the total number of spatial directions were two, rather than the three we experience daily. This may not seem important for a non-theoretician, but in the language of the AdS/CFT-correspondence we introduce later, it is.

It is also worth mentioning that due to the close relationship between the dielectric function and the conductivity (2.16), observations of the latter can be used to find dispersion relations for collective modes. It is thus a simple matter to verify that the conductivity found in e.g. [17] also yields the characteristic $\omega \propto \sqrt{k}$ dispersion, even though that particular computation is carried out for the Dirac fluid phase of graphene, which is strongly coupled - i.e. the arguments in the previous section does not hold.

The same relation has also been found in other studies with conventional condensed matter techniques such as random phase approximations (RPA) and self-consistent field approximations [18, 19].

The 2D plasmon dispersion has also been experimentally observed in graphene e.g. [20–22].

While the 3D bulk plasmon for metals is well studied experimentally, it has only recently been partly available to observe experimentally in strange metals with momentum-resolved electron energy-loss spectroscopy [23].

Chapter 3

Strange metals

In this chapter we will discuss some of the problems arising due to strong coupling in certain materials, often called strange metals.

In the previous chapter we treated electrodynamical response in some classical models. With a weak electromagnetic coupling strength, these model works well (for the purpose of this thesis at least). Quantum mechanically, the coupling strength has many interpretations, but the most clear one is a proportionality to how likely a charged particle is to emit or absorb a photon. This can in turn be expressed in terms of Feynman diagrams, where such an interaction is of the form of a particle going in to the interaction point, and a particle and a photon going away. The likelyhood of each such vertex is related to the bare coupling strength, meaning that for a small interaction strength, diagrams with more vertices are less likely, and may at some point be negligible. For small coupling strength, it is therefore relevant to consider expansions in the coupling parameter, where to get some arbitrary precision, you can include all possible diagrams with up to n vertices, as essentially other diagrams are suppressed by order α^n, which is very small, and thus gives rise to a very small error. This is the fundament of perturbation theory, which is one of the most successful tools used in condensed matter theory. In a vacuum, the electromagnetic coupling strength is about $1/137$, which is definitely small enough for perturbation theory to provide an accurate description.

However, in many theories one is not that fortunate. Remarkably, this is not a problem as often as one would initially expect. For instance in most metals, the coupling strength is about order one, which would imply that the higher order terms would not be negligible to any expansion order. Due to a very fortunate circumstance, they are often able to be described with Fermi-Landau theory as Fermi-liquids. Liquid here being a keyword implying that they are strongly coupled, but essentially still a continuation of the weakly coupled electron gas. This holds essentially because the theory works at small coupling strengths, and while continuously turning up the

coupling constant from small values, the theory passes no poles, no phase transition occurs and one would thus expect a similar behaviour [24].

However, as stated above, this is not what one would have expected but rather a common, but fortunate case. Metals could just as well have had a phase transition, which would leave us in the dark about how the next phase worked. What we know is that it is found were one would ordinarily expect a metallic phase, but the excitations are not well described by the electron-hole pair quasi-particles of Fermi-Landau theory. And from this follows the fitting name of "strange metals".

Although quantum field theory struggles to describe these phases, there has been some success with the random phase approximation (RPA) method. In this method, one argues that, largely from symmetries, that many of the contributions from the diagrams can be neglected due to cancellations. Instead a specific sequence of diagrams are summed, which can analytically be summed, specifically the sequence presented in figure 3.1.

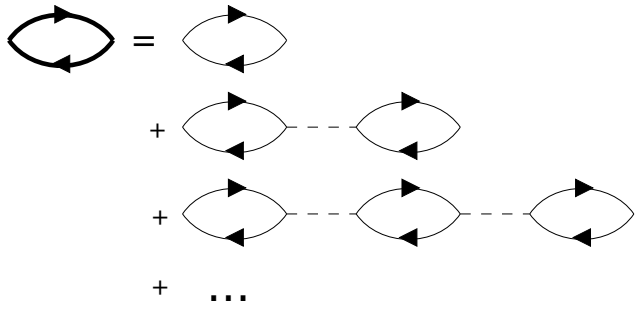

Figure 3.1: Feynmann diagrams summed in the RPA. On the left side, in bold, is the full Green's function, and on the right side the non-interacting Green's function as lines and the interaction photon dashed.

In terms of the interaction potential V, and the screened correlator χ_{sc}, the full correlator χ is given as

$$\begin{aligned}\chi(\omega, \boldsymbol{k}) &= \chi_{sc} + \chi_{sc} V \chi_{sc} + \chi_{sc} V \chi_{sc} V \chi_{sc} + \dots \\ &= \frac{\chi_{sc}(\omega, \boldsymbol{k})}{1 - V(\omega, \boldsymbol{k}) \chi_{sc}(\omega, \boldsymbol{k})} \,. \end{aligned} \tag{3.1}$$

This expression is in fact closely related to the similar relation in (2.21), as the denominator in (3.1) becomes the dielectric function via (2.20) and (2.16). Although RPA is primarily used for weak coupling, where the convergence can be argued, it has also had some limited success for strongly coupled systems, where the motivation behind the approximation somewhat falls short.

However, where the usefulness of conventional condensed matter methods is limited, holography steps up as an exceptional candidate to make

theoretical descriptions and predictions of such phases. This has been an endeavor for some time now [25] and has been remarkably successful [26, 27].

There are primarily two different types of strange metals observed, and they are in some ways related. High temperature superconductors display that behaviour at temperatures above the superconducting phase, and graphene [28] (and possibly other newly discovered 2D materials) when doped to near charge neutrality. As the high temperature superconductors are layered materials, they are dimensionally related, even though one of them is a bulk material (i.e. 3D) and the other a sheet.

3.1 High temperature superconductors

High temperature superconductors are materials that become superconducting at temperatures below some critical temperature T_c, that is large compared to what could be expected from BCS-theory, about 30 K. Where there is still no comprehensive theoretical understanding of this phase, there exist partial descriptions, such as resonating valence bond theory. One important observation is however that the mechanism is not an electron-phonon interaction as in BCS-theory, but rather some electronic coupling which varies between different materials.

After the discovery of the first high temperature superconductor, almost all high temperature superconductors for twenty years were variations of that one, layered materials of metallic elements and copper oxides, referred to as cuprates. Today there are also iron based superconductors as the second large group of superconductors, and a few oddballs, such as hydrogen sulfide under extreme pressure.

At temperatures above T_c, cuprates are in the strange metal phase, which is even less well understood than the superconducting phase. This phase displays several intriguing properties, such as Planckian dissipation, T-linear resistivity and minimal viscosity [29, 30]. This phase is characterized by strong coupling, long-range entanglement and cannot be described by quasiparticles. This essentially cripples conventional condensed matter tools such as perturbation theory and Monte-Carlo methods, but paves the way for a holographic treatment.

3.2 Graphene near charge neutrality

Graphene is as close to perfectly two-dimensional a material can get. A single atom thick, it is a sheet of carbon atoms, arranged in a hexagonal, honeycomb structure. This has some very important ramifications for its properties. Graphene is, despite being thin, incredibly strong and durable. It also has some very interesting electrical properties; it conducts incredibly well, but can be doped to display even further exotic behaviours. There

appears to be innumerable reasons to study graphene, and it turns out strong coupling is another one.

Although it was in the 21st century graphene was discovered and received attention, it is actually an old theoretical construction, with a model treatment as early as 1920 by Wallace [31]. As graphite has been common knowledge to be multiple weakly connected layers of carbon, a single sheet is a rather natural construction and exactly what graphene is.

Although a theoretical description was available, it took 84 years before Novoselov and Geim produced it and verified that they had indeed found graphene. They were subsequently rewarded with a Nobel prize for their discovery in 2010, and an immense amount of research has since gone into the newly born field of graphene physics. For instance, the European Union started their flagship, investing billions into the vision of graphene being available to consumers by 2025, with Chalmers University of Technology as its base.

As many materials with extreme and exotic properties, graphene has some very interesting potential applications. Because it is thin, miniaturization of circuits. Because it is flexible, bendable electronics. Because it is strong, as discrete reinforcement, and many more.

For the purpose of this thesis, graphene is especially interesting for two reasons. Firstly, there is the Dirac point. At a specific level of doping, the Fermi surface of graphene vanishes, and all electrons are instead bound to their respective nuclei. This results in an effectively neutral system. Near this point, graphene has shown indications of strong coupling, making holography an excellent framework to treat the system [28].

Secondly, the 2-dimensional nature of graphene has some very interesting implications as well as being the underlying fundament to its other properties. It is a quite natural extension to go from a treatment of 3D plasmons to a treatment of 2D plasmons, which is done in paper II.

Chapter 4

Holography

Holography is one of those things in physics that for the uninitiated may seem like witchcraft, and possibly even to those in the field.

The underlying principle is that of a duality, between a QFT and a gravity theory in a larger space. The key interest lies in that one of them can be strongly coupled (usually chosen to be the QFT) while the other is weakly coupled. Then, on the QFT side, we have a theory that is remarkably complex, and practically impossible to treat mathematically, even with the most powerful computers. On the other side, we have something seemingly unrelated and comparatively simple that we have little trouble making calculations and predictions for. The duality makes the bold claim, that they can both be governed by the same dynamics, and the results from one side, can be translated to the other.

The duality has since it's inception grown to encompass a lot more than it's original formulation, and has with increasing generalization and different target applications earned many different names. Most of these are still in use - from the very specific "AdS/CFT-correspondence" as the gravity side should asymptotically be a negatively curved anti-de Sitter (AdS) space, and the other side a conformal field theory (CFT) - to the less specific "gauge/gravity duality" simply denoting what type of theory is on each side - to the very broad name of "holography" indicating a more hands on approach that we project one theory into a larger space, precisely like a hologram. This increasing generality also means less constraints on the QFT, making the duality more enticing for condensed matter theory.

In recent years, several excellent books on the subject have been written for the reader that wants to get into the subject [32–34].

4.1 History

Symmetries have throughout mankind's history always had an almost mythical presence. In art, many forms strive for symmetry, and others strive to

break symmetries for dramatic effects. In society, we see symmetries as a naturally just system, worthy of pursuit. Similarly, symmetries play an intuitive but crucial role in physics. The force exerted by one object onto another is returned with identical size but opposite direction. Gravitational and electromagnetic forces only depend on the distance to an object, resulting in spherical symmetries. Also less obvious, but fundamental symmetries of time and space, if you conduct an experiment (under similar circumstances) it does not matter when or where you conduct the experiment, the very cornerstone of science itself.

The pursuit of symmetries in physics can seem almost maniacal, but as records show, has been correspondingly successful. Both in that there is an intricate relationship between conserved quantities and symmetries (Noether's theorem) – conserved energy corresponds to a time symmetry, conserved momentum to translational symmetry, and many more. Even the fundamental forces of nature corresponds to different symmetries. A lot of theoretical physics is based around understanding symmetries, and the effects of spontaneously or explicitly breaking these symmetries, and has been the driving force behind theories such as supersymmetry, which very naturally occurs in string theory, but not apparently at our energy scale in daily life.

As different physical theories are fundamentally described by their symmetries, different theories with the same symmetries behave very similarly, regardless of how these symmetries arose. This leads to the notion of dualities, where simply describing one system is enough, and where you can translate the results from that system to others that have the same symmetries. Especially in string theory these are prevalent, as the underlying framework has a lot of symmetries (literally supersymmetric), and you can achieve different symmetries by simply breaking some symmetries rather than having to introduce new ones.

There are many important and famous dualities in string theory, but none more so than the AdS/CFT-correspondence, discovered by Maldacena in 1997 [35]. Maldacena noted that the symmetries of the boundary of an anti-de Sitter space in a weakly coupled string theory, mirror the symmetries of a strongly coupled conformal field theory, in particular an SU(N) super Yang-Mills theory for large N, similar to what dominates the rather poorly understood quark-gluon plasma of quantum chromodynamics (QCD).

The discovery was remarkable in it's own merit, but it wasn't until the incredible, verifiable predictions of the strongly coupled quark-gluon plasma [36] that the discovery got real attention from non-theorists. Another significant increase of interest came with exceptional agreements from weakly coupled AdS-spaces to strongly coupled condensed matter field theory (AdS/CMT, that is dualizing with an electromagnetic theory) as the applications in condensed matter physics are not only there, but the need for some way to describe strange metals exists, as well as the huge potential

gains of understanding and predicting their behaviours.

Although the original duality was formulated in string theory, it can also be derived within ordinary gravity ordinary gravity theories [37]. In those situations, there are however no guarantees that the theory is quantum consistent, which is a property that dualities derived from string theory naturally inherits from string theory and is highly relevant for "quantum matter".

4.2 Models

The way Maldacena introduced the duality has become known as a top-down perspective. The idea here is to take everything you want from the field theory (which we will also call the boundary theory) and include it in a string theory setup, building up a complex gravitational theory, that very accurately describes the known boundary theory. Another, different approach is that, since the boundary theory one wishes to describe in the CMT, is not an SU(N) with large N, one might as well take a known bulk theory, and see what it describes on the boundary. These are known as bottom-up models, and they have the benefit that bulks that are simpler can be perturbed in a manner to include various concepts that would otherwise be rather difficult to include in a controlled top-down manner.

One effect that is difficult to include in a top-down model is a dynamical metric. To include such effects, one would need to include how the presence of D-branes would back-react the metric. This significantly complicates top-down models relative to the commonly used probe brane models where, under the assumption that the number of probe branes is very small, back-reaction can to some extent be neglected. In general, such probe-brane systems have been quite successful, but for the application of collective modes, the dynamical gravity effects of the embedding appears insufficient to model plasmons and collective modes.

Thus, in this thesis, we exclusively treat bottom-up systems.

4.3 Bulk Theory

The strongly coupled QFT and the weakly coupled gravity theory are linked together by a "geometrization" of the renormalization group scale of the QFT. This essentially means that one introduces a new "energy dimension" to the QFT, and in that extended spacetime the gravity theory lives. This naturally gives a notion of a *boundary* theory (the QFT) and a *bulk* theory (the gravity theory).

In the other end of the energy dimension, one finds a black hole. This black hole corresponds to the temperature of the boundary theory, where the black hole has a matching Hawking temperature. It should be noted

however that the black hole has an infinite extension, unlike black holes astronomers may find. A "real" black hole is in this setting referred to as a spherical black hole, i.e. it located at some point and extends some distance away to what is known as its horizon. A holographic black hole is infinitely extended in all dimensions but the energy one, and extends some (finite) distance also in that one. If the boundary has two spatial directions, the black hole is located on a mathematical plane and is thus called *planar*, as pictured in figure 4.1. As such, it would arguably be more fitting to refer to them as black planes, or as is done in string theory, black branes. We opt, as is often done, to keep the familiar terms, even in calling the distance to the black hole a radial distance.

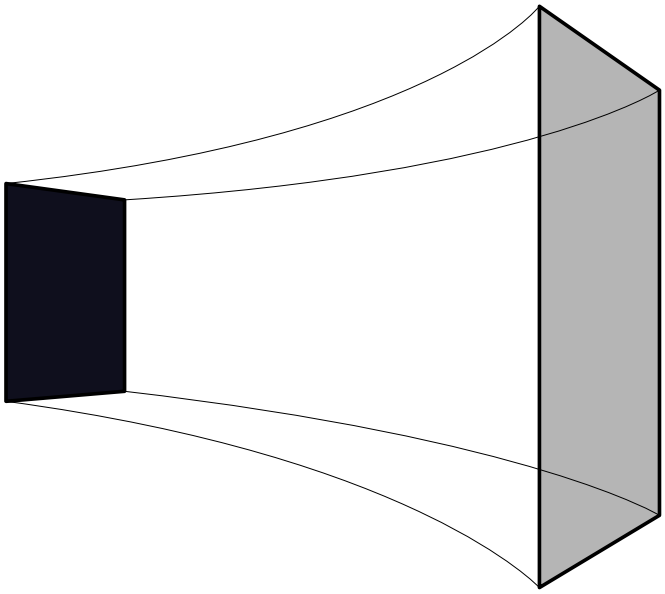

Figure 4.1: The basic holographic setup. To the left, at the "bottom" is a (planar) black hole, and the gray surface to the right is referred to as the boundary. The volume in between is referred to as the bulk.

A non-zero chemical potential on the boundary, is similarly reflected in the charge of the black hole, and can be read off as the boundary value of the gauge potential in the bulk. Other quantities of the boundary theory can similarly translated from the bulk theory, according to what is commonly referred to as the holographic *dictionary*.

The essence of this dictionary is formally captured in the Gubser-Klebanov-Polyakov-Witten (GKPW) formula, which equates the generating functional of the boundary theory to the partition function of the bulk theory,

$$Z_{QFT}[\{h_i(x)\}] = Z_{Gravity}[\{h_i(x)\}]. \tag{4.1}$$

That is, the generating function of an operator $\mathcal{O}_i$ with source h_i in the

boundary theory,

$$Z_{QFT}[\{h_i(x)\}] \equiv \left\langle e^{i\sum_i \int dx h_i(x)\mathcal{O}_i(x)} \right\rangle , \tag{4.2}$$

matches the partition function of the bulk theory with a bulk field ϕ_i, corresponding to $\mathcal{O}_i$, which takes the boundary value h_i

$$Z_{Gravity}[\{h_i(x)\}] \equiv \int^{\phi_i \to h_i} \left(\prod_i \mathcal{D}\phi_i \right) e^{iS[\{\phi_i\}]} . \tag{4.3}$$

This is visually represented in figure 4.2.

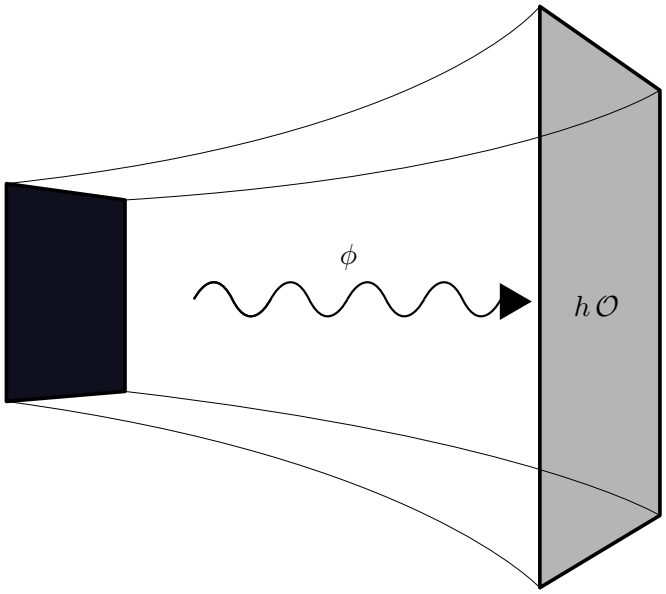

Figure 4.2: The holographic dictionary: A bulk field ϕ's boundary value h, is the source of a QFT operator $\mathcal{O}$. As an example, a bulk electric flux from a charged black hole yields a charge density in the boundary theory.

The temperature and chemical potential are in many ways the fundamental building blocks for a holographic description. In the bulk, they are linked together via the Einstein-Maxwell action with a cosmological constant, Λ, that ensures the asymptotic AdS geometry. This yields the familiar Lagrangian

$$\mathcal{L}_{ME} = -\tfrac{1}{4}F_{\mu\nu}F^{\mu\nu} + \tfrac{1}{2}(-2\Lambda + R), \tag{4.4}$$

where R is the Ricci scalar found in general relativity and we have chosen to work in natural units[1].

[1]That is, units chosen such that most physical constants, such as the speed of light, are one

Varying the action (4.4) with respect to the metric g and the gauge potential A yields a set of equations of motion which can be solved to find the values of the respective fields at any given point and time. These are obtained as

$$0 = -\nabla_\kappa \nabla^\kappa A^\mu + \nabla_\kappa \nabla^\mu A^\kappa \,, \tag{4.5}$$

$$0 = -\Lambda g^{\mu\nu} - \tfrac{1}{4} g^{\mu\nu} F_{\kappa\lambda} F^{\kappa\lambda} + F^{\mu\kappa} F^{\nu}{}_{\kappa} - R^{\mu\nu} + \tfrac{1}{2} g^{\mu\nu} R \,. \tag{4.6}$$

4.3.1 Background solution

As it is by far the most convenient to work in linear response, we first need to solve for a background and secondly solve for a small perturbation around that background.

While it is also possible to study systems at zero temperature, we opted to study cases with non-zero temperature, which are experimentally most relevant. This allows us to define our coordinate system with the "radial/energy" coordinate z such that the black hole's event horizon is located at $z = 1$ and the boundary is located at $z = 0$. This effectively means redefining the coordinates as $z = r_H/r$ in the more conventional coordinate system where $r = r_H$ is the location of the black hole horizon and the boundary is located at $r \to \infty$.

We assume the background to be static (unchanging in time), and in the spatial directions, homogeneous and isotropic (unchanging with position and similar in all directions). In a $(3+1)$-dimensional bulk we can make an ansatz for the metric as

$$L^{-2}\,\mathrm{d}s^2 = L^{-2} g_{\mu\nu}\,\mathrm{d}x^\mu x^\nu = -f(z)\,\mathrm{d}t^2 + z^{-2}\,\mathrm{d}x^2 + z^{-2}\,\mathrm{d}y^2 + g(z)\,\mathrm{d}z^2, \tag{4.7}$$

where f and g are functions of the radial coordinate z, and L is the AdS length scale,

$$\Lambda = -\frac{3}{L^2} \,. \tag{4.8}$$

Motivated by isotropy, we can also make an ansatz for the Maxwell gauge field A to only point in the time-direction, i.e.

$$A_\mu = L \begin{pmatrix} h(z) & 0 & 0 & 0 \end{pmatrix} . \tag{4.9}$$

Inserting these assumptions into (4.5) and (4.6) yields three scalar equations of motion,

$$0 = 4fg + gzf' + fzg' \,, \tag{4.10}$$

$$0 = -2f + 6fgz^2 + 2zf' - z^2\big(h'\big)^2 \,, \tag{4.11}$$

$$0 = h'' \,, \tag{4.12}$$

where prime denotes a radial derivative. These are solved by

$$f(z) = \frac{c^2}{z^2} - Mz + \frac{1}{2}Q^2z^2\,, \tag{4.13}$$

$$g(z) = \frac{c^2}{z^4 f(z)}\,, \tag{4.14}$$

$$h(z) = \mu - Qz\,, \tag{4.15}$$

meaning that the background has four free parameters, c, M, Q and μ. The chemical potential μ is fixed by requiring the Maxwell potential to disappear on the horizon,

$$h(1) = 0 \Rightarrow \mu = Q, \tag{4.16}$$

which would otherwise cause a gauge singularity. As we have rescaled the radial coordinate to have the horizon at $z = 1$, this in turn sets a restriction on the mass,

$$f(1) = 0 \Rightarrow M = c^2 + \frac{1}{2}Q^2. \tag{4.17}$$

The speed of light is set by our choice of units,

$$c = 1. \tag{4.18}$$

This leads to a single parameter Q corresponding to the charge of the black hole, that defines the background.

This is the simplest possible bulk model to study holographically. The solution is a planar charged black hole – a Reissner-Nordström (RN) black hole. The boundary theory is referred to as an RN-metal, which should be noted is only a well defined theoretical matter, but it should be a fairly good description of many strongly coupled electron gasses.

It is worth mentioning here that we have chosen the bulk theory to be $(3 + 1)$-dimensional, which means the boundary will only have two spatial coordinates (with time being the "+1"). This may seem more natural for studying surface modes than modes in a bulk, where the charges would normally be free to move in three spatial directions. This is done primarily to simplify things, as in one additional dimension, the Maxwell field exhibits a logarithmic divergence at the boundary. This can be carefully regularized, but those extra steps are not expected to yield significantly different results. Thus it is common to avoid them by studying a (2+1)-dimensional boundary theory, which is what we have chosen to do here.

4.3.2 Perturbation solution

Having solved the relatively simple background, we now turn to a perturbation of this background. The purpose of this is to analyze the dynamics in linear response. The dynamics are otherwise rather difficult and computationally expensive to compute in their full non-linear glory. Working in

linear response however, we assume that the changes are small relative to the background. This means that if the perturbations are of order ε, then we can neglect any terms of order ε^2 and higher, since they would then be very small.

This also allows us to Fourier transform our eventual solution meaning we can analyze individual wavelengths and frequencies from the start. Without loss of generality, we assume the wave to travel in the x-direction, which implies that the time and spatial dependence (on non-radial coordinates) will be $\propto e^{-i\omega t+ikx}$, where we have introduced ω as the angular frequency and k as the wavenumber.

Since the theory is invariant under diffeomorphisms, we can choose to work in radial gauge, i.e. the components $\delta g_{\mu z}$, $(\mu = t, x, y, z)$ and δA_z can be set to zero. Also, as the background is invariant under parity, $y \to -y$, we can chose to study the longitudinal (δg_{tt}, δg_{tx}, δg_{xx}, δg_{yy}, δA_t, δA_x) and transversal (δg_{ty}, δg_{xy}, δA_y) response separately. In this thesis we focus on the longitudinal sector as modelling plasmons is the primary aim.

Put together, this means we perturb with

$$\delta g_{\mu\nu} = \varepsilon L^2 e^{-i\omega+kx} \begin{pmatrix} \delta g_{\mathrm{tt}}(z) & \delta g_{\mathrm{tx}}(z) & 0 & 0 \\ \delta g_{\mathrm{tx}}(z) & \delta g_{\mathrm{xx}}(z) & 0 & 0 \\ 0 & 0 & \delta g_{\mathrm{yy}}(z) & 0 \\ 0 & 0 & 0 & 0 \end{pmatrix} \tag{4.19}$$

and

$$\delta A_\mu = \varepsilon L e^{-i\omega+kx} \begin{pmatrix} \delta A_t(z) & \delta A_x(z) & 0 & 0 \end{pmatrix} . \tag{4.20}$$

Perturbing the background solution, i.e. $g_{\mu\nu} \to g_{\mu\nu}+\delta g_{\mu\nu}$ and $A_\mu \to A_\mu + \delta A_\mu$ equations (4.5) and (4.6) become vastly more complex than previously. However, since we are considering linear response we can discard terms of order ε^2 and higher, drastically simplifying the system. Furthermore, order ε^0 is already solved by the background solution.

We are left with a system of six coupled second order linear ODEs (from the g_{tt}, g_{tx}, g_{xx}, g_{yy}, A_t and A_x components) as well as four constraint equations (from the g_{tz}, g_{xz}, g_{zz} and A_{zz} components) that serves as a check, as they should hold true if we could actually make the choice of radial gauge we made above. The equations are still rather lengthy, but are included in appendix A for the curious reader.

These equations cannot be solved analytically, and have to be solved numerically. The form of the background provides a specific challenge for a numerical solution as the horizon needs to be addressed. There are multiple ways of dealing with this. From a theoretical standpoint, a coordinate switch to Eddington-Finkelstein coordinates solves the issue, but from a practical standpoint, it is more convenient to factor out an exponential term in the fields and in the equations amounting to a Frobenius expansion. This factor

is frequency dependent, and explicitly one gets near the horizon

$$\delta A_t = (1-z)^{\pm\frac{2i\omega}{6-Q^2}}\delta A_t^*\,, \qquad (4.21)$$
$$\dots$$

where the star indicates the (regular) field post Frobenius expansion. Both the positive and the negative exponent correspond to mathematical solutions, but only the negative one yields *physical* solutions as they can be interpreted as out-going and in-falling solutions, of which only the latter is sensible in regards to a black hole.

In the process of expanding the fields, the singular behaviour of f and g eliminates multiple degrees of freedom. Six coupled second order ODE's are expected to be defined up to initial values of each field and their first derivative, i.e. twelve degrees of freedom, of which one eliminates half by requiring in-falling boundary conditions. Thus, one would still naively expect to have six degrees of freedom left, but in this case, there are only two – the others have been eliminated by the singular behaviour at the horizon. The two remaining degrees of freedom can be chosen to be $\delta A_x^*(1)$ and $\delta g_{xx}^*(1)$.

There are in fact four more solutions that are missed in the treatment above. They are pure gauge solutions from the remaining degrees of freedom in our gauge choice, and as such do not need to fulfill the above mentioned requirements. These are solutions of the form

$$\delta g_{\mu\nu} = \nabla_\mu \xi_\nu + \nabla_\nu \xi_\mu \qquad (4.22)$$
$$\delta A_\mu = \xi^\nu \nabla_\nu A_\mu + A_\nu \nabla_\mu \xi^\nu\,, \qquad (4.23)$$

and

$$\delta A_\mu = \nabla_\mu \zeta\,, \qquad (4.24)$$

for some ξ or ζ. A similar treatment is made in [38]. These solutions can be found analytically, but we do not include them here as some are quite long.

Thus, there are six linearly independent solutions, and any linear combination of these is also a solution to the equations of motion. To get a unique solution, one needs to implement six additional boundary condition at the conformal boundary.

4.4 Boundary conditions

The boundary conditions to enforce on the conformal boundary are closely related to the boundary theory itself. In a sense, the parameter Q and the horizon radius r_H that we eliminated from the equations by changing our coordinate system are also determined by the boundary theory. They are both closely related to the temperature and the chemical potential of the boundary theory.

The (Hawking) temperature can be identified by Wick rotating. Near the horizon, the Euclidean time is periodic with the inverse temperature as period, leading to

$$T = \frac{6 - Q^2}{8\pi} \frac{r_H}{L} \,. \tag{4.25}$$

The holographic dictionary identifies the boundary field strength $\mathcal{F}$ and the boundary current $\mathcal{J}$,

$$\mathcal{F} \;=\; \frac{1}{\sqrt{\lambda}} F\big|_{\partial M} \,, \quad \mathcal{J} \;=\; \sqrt{\lambda}\, \imath_n W\big|_{\partial M} \,, \tag{4.26}$$

from the bulk field strength F and the bulk induction tensor W (composed by $\boldsymbol{E}, \boldsymbol{B}$ and $\boldsymbol{D}, \boldsymbol{H}$ respectively). Here we have introduced the parameter λ which relates the coupling strength for electromagnetism on the boundary theory with the one in the bulk. They do not necessarily have to be equal (which would correspond to $\lambda = 1$). This ultimately leads to

$$\mu = \frac{Q}{\sqrt{\lambda}} \frac{r_H}{L} \,. \tag{4.27}$$

That means, given a specific chemical potential μ and a temperature T on the boundary, there exists values of r_H and Q in a the bulk that yields those values on the boundary. As the horizon radius does not enter into the ODE's we solve, it is convenient to use the dimensionless quantity μ/T on the boundary to describe different boundary theories as it only depends on Q.

This means that (up to rescaling), all RN-metals at the same μ/T behave similarly. Furthermore, the charge density can also be uniquely determined from the holographic dictionary by the chemical potential and the temperature for all such systems,

$$n \;=\; \sqrt{\lambda}\, Q \frac{r_H^2}{L^2} \;=\; \frac{2}{3}\pi\lambda\mu T + \frac{1}{6}\lambda\mu\sqrt{6\lambda\mu^2 + 16\pi^2 T^2} \,. \tag{4.28}$$

This constraint is not necessary for most boundary theories, so to model more realistic systems one needs to include another scale into the system, something that is done in e.g. the electron cloud model we look at in section 4.6.

Similarly, the boundary conditions on the perturbations can be found from properties of the boundary theory. Most notably, since there is no dynamical gravity in the boundary theory (gravitational effects are generally negligible in relevant QFT-duals), the perturbations of the four metric components should vanish on the boundary.

Similar to how the background field gives rise to a potential and a charge density, the perturbations gives rise to fluctuations in these. With bulk[2]

[2]The "bulk" here refers to the entirety of the CMT as in chapter 2, not to be confused with the bulk of the holographic model.

plasmons (or collective modes) in mind, the aim is for a realization of (2.24) and for 2D plasmons (2.29).

With the holographic dictionary (4.26), the bulk plasmon condition (2.24) and $\phi = 0$ gauge corresponds to boundary conditions

$$\left(\omega^2 \delta A_x + \lambda \delta A_x'\right)\Big|_{\partial M} = 0\,, \qquad \delta A_t\Big|_{\partial M} = 0\,, \tag{4.29}$$

and the 2D plasmon condition (2.29) to

$$\left(\omega^2 \delta A_x + \lambda \frac{|k|}{2} \delta A_x'\right)\Big|_{\partial M} = 0\,, \qquad \delta A_t\Big|_{\partial M} = 0\,. \tag{4.30}$$

Given that the dynamics of the boundary theory is described in terms of electrons and photons, these "mixed" boundary conditions are especially reasonable, as Witten argues that Neumann boundary conditions (only the primed term) would yield a dynamical photon on the boundary [39].

Quasinormal modes would similarly correspond to

$$\delta A_x\Big|_{\partial M} = 0\,, \qquad \delta A_t\Big|_{\partial M} = 0\,, \tag{4.31}$$

both for bulk and 2DEG systems.

These boundary conditions can also be related to what is known as "double trace deformations" and an RPA form of the Green's function [33, 40, 41].

The quasinormal modes of the system have been studied before, in e.g. [42, 43] and in the context of neutral plasmas, the collective modes were studied in [44].

Once a complete set of boundary conditions has been chosen, one can start looking for solutions to the full boundary value problem. It is worth noting that as the equations of motion are linear and homogeneous, and the boundary conditions themselves are also homogeneous, the trivial solution (i.e. all fields are zero) is always a possibility. This solution is of course not the desired one, but it does convey an important message – there does not exist a non-trivial solution to the boundary value problem for any ω and k. In fact, what is actually sought after is for what values of ω and k there do exist non-trivial solutions. There exists a non-trivial solution if the six boundary values of the six linearly independent solutions are not linearly independent. This is most conveniently examined by evaluating the determinant of the corresponding 6×6-matrix – if they are linearly dependent, it is zero.

$$\left|\begin{array}{cccccc} (\delta g_{\mathrm{tt}})_1 & (\delta g_{\mathrm{tx}})_1 & (\delta g_{\mathrm{xx}})_1 & (\delta g_{\mathrm{yy}})_1 & (\delta A_{\mathrm{t}})_1 & (\omega^2 \delta A_{\mathrm{x}} + \delta A_x')_1 \\ (\delta g_{\mathrm{tt}})_2 & (\delta g_{\mathrm{tx}})_2 & (\delta g_{\mathrm{xx}})_2 & (\delta g_{\mathrm{yy}})_2 & (\delta A_{\mathrm{t}})_2 & (\omega^2 \delta A_{\mathrm{x}} + \delta A_x')_2 \\ & & & \cdots & & \end{array}\right|_{z\to 0} = 0, \tag{4.32}$$

As the calculations are done numerically, one needs to specify some sufficiently strong precision.

Procedurally, this is rather straight forward:

- Choose a background, i.e. μ/T.
- Choose a wave number k.
- Guess a (complex-valued) ω.
- Compute the six linearly independent solutions to the equations.
- Examine if there is a non-trivial linear combination of these solutions, i.e. compute the determinant.
- Make a better guess of ω, repeat until chosen precision is achieved.

These are the systems that are considered in paper I-III

In paper I the general framework of collective modes in holography is worked out, and in paper III the analysis is further extended for bulk plasmons.

In paper II the 2D plasmon condition is considered.

4.5 Other holographic quantities

It is worth mentioning that several properties of the system are only available when not imposing the full set of boundary conditions. For instance, a computation of the conductivity is a computation between the ratio of the electric field and the induced current on the boundary. If, for QNMs, one imposes Dirichlet boundary conditions on the electric field (i.e. zero), such a ratio would be nonsensical. However, imposing the other boundary conditions allows us find a linear combination of the six solutions for any given (ω, k), unless specifically chosen on a QNM, which can be used to compute the conductivity of the boundary system. This also then naturally yields the dielectric function via (2.16), and in this particular sense, the dynamic charge response has previously been studied in [45, 46]. It is also especially useful when comparing to experiments, since in experiments one rarely probes at the exact, complex wavenumber and frequency. Instead, what is typically done is to sweep over a range of values and plot spectral functions. This can thus also be done holographically, although as it is less mathematically interesting it is often omitted. Similarily, computations of the conductivity and dielectric function can be used to verify specific "sum rules" that all materials should satisfy [47].

4.6 The electron cloud

The RN bulk model that has been covered previously is a rather simple model, and may for some considerations be just a bit too simple.

The fact that we cannot tune temperature, chemical potential and charge density as three independent parameters and effectively only have one parameter is an apparent weakness. To address this, one would need to implement two additional scales in the system.

Another important note is that if the bulk theory supports charged particles, the RN black hole is unstable [48–50]. If the temperature of the black hole is decreased (Q is increased), the local chemical potential in the bulk is eventually large enough to support a density of such charged particles, leading to pair production and hence an instability. The extremal solution ($Q = \sqrt{6}$) is then never reached. This is in essence a good thing; the extremal solution has other problems which arise when there is effectively a double event horizon. However, it does mean that the static RN bulk background is not sufficient at low temperatures. This feature is well established and if the particles are charged scalars, the bulk scalar condenses at low temperatures, which is what results in holographic superconductors [51, 52].

If instead the charged particles in the bulk theory are fermions, the bulk may for large enough Q support a density of those at a distance outside of the horizon, as in figure 4.3. We refer to such a setup as an "electron cloud". It is worth noting that these charged particles are not the same as the electrons on the boundary, but merely a name reflecting their nature. Gradually decreasing the temperature increases the extent of the cloud and ultimately, the bulk collapses into an "electron star", which has several similarities to a neutron star.

That collapse is however of limited interest here for several reasons. Firstly, if the bulk also supports a scalar of greater mass, then that would also contribute at low temperatures. Secondly, for lower temperatures of the black hole, the temperature of the electron cloud becomes increasingly important. From a computational perspective, this is non-trivial as one of the most important simplifications typically done is to assume that the cloud is cold. This makes the inner and outer limit of the cloud seen in figure 4.3 well defined. Instead, having a Fermi-Dirac distribution of the particles in terms of the local chemical potential would mean that for any non-zero temperature of the cloud, the cloud would stretch all the way from the horizon to the conformal boundary. This causes a wide range of difficult issues, including the need for a radiative description of the black holes collapse. Thirdly, by keeping the previous description of the RN hole, we indirectly close the door of such a collapse as we normalize with the horizon radius, which would not be applicable in a system without a black hole.

But as a first step in such a mode of instability, the electron cloud is an interesting model. Furthermore, the mass and charge of such fermions in-

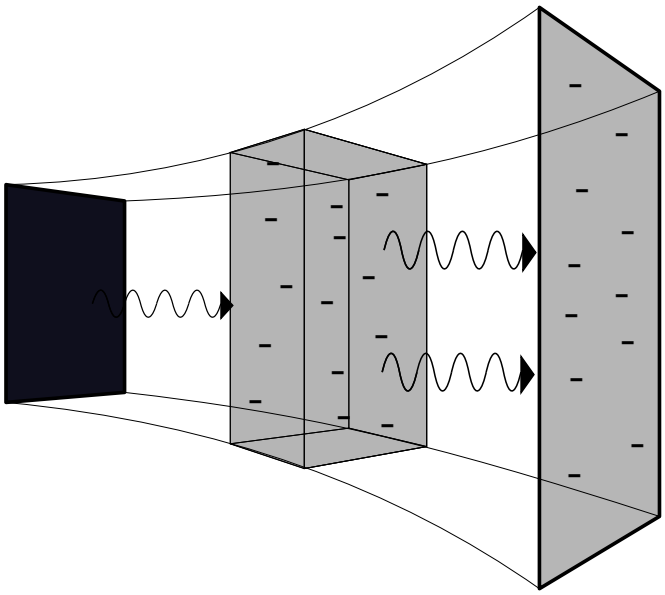

Figure 4.3: The electron cloud bulk. If the mass of the charged fermion and the temperature of the black hole is sufficiently low, there will exist a region between the black hole and the boundary in which a density of fermions are supported.

troduce two additional scales which would allow us to tune the temperature, chemical potential and charge density of the boundary system independently.

The Einstein-Maxwell action (4.4) is for the electron cloud extended with the Lagrangian of a charged, non-rotating, zero temperature, perfect fluid [53],

$$\mathcal{L}_{fl} = -\rho_{\text{fl}}(n) + nu^{\mu}A_{\mu} + nu^{\mu}\partial_{\mu}\phi + \lambda\left(1 + g_{\mu\nu}u^{\mu}u^{\nu}\right) , \tag{4.33}$$

where ρ_{fl} and n is the energy density and number density respectively. The charge of the fluid particles has been set to unity. ϕ is a 'Clebsch' potential that ensures that the mass of the fluid is conserved. Similarly, λ is a Lagrange multiplier implementing that u^{μ}, the local fluid velocity, squares to minus one, as required for the 4-velocity.

The local chemical potential in the bulk is then

$$\mu_{loc} = u^{\mu}\left(A_{\mu} + \partial_{\mu}\phi\right) . \tag{4.34}$$

It should be mentioned that this local chemical potential in the bulk can also be used outside the electron cloud, as it is the factor n that makes the contribution to the Lagrangian vanish, meaning that it is a well defined quantity even for the pure RN solution (the contribution from the 'Clebsch' potential will however vanish). The cloud is supported when the local bulk chemical potential is larger than the mass of the fermions, m.

Approximated in the Thomas–Fermi limit, the density of states is

$$D(E) \;=\; \beta E\sqrt{(E^2-m^2)}\,, \tag{4.35}$$

for energies above the cloud particle mass m, and where β is a parameter determining the density of the cloud, not to be confused with the β in chapter 2. This sets the number density and the energy density inside the cloud as

$$n \;=\; \int_m^{\mu_{loc}} D(E)\,\mathrm{d}E\,, \qquad \rho_{fl} \;=\; \int_m^{\mu_{loc}} E\,D(E)\,\mathrm{d}E\,, \tag{4.36}$$

respectively. The pressure is then given by the usual equation of state,

$$p \;=\; -\rho_{fl} + n\mu_{loc}\,. \tag{4.37}$$

Variations with respect to the introduced fields in most cases correspond to algebraic constraints, which can directly be used to eliminate fields from the equations of motions which need to be solved. The background solution for u is

$$u^\mu = L^2\left(\;\sqrt{f(z)},\quad 0,\quad 0,\quad 0\;\right), \tag{4.38}$$

with the longitudinal perturbation

$$\delta u^\mu = \varepsilon L^2 e^{-i\omega t+ikx}\left(\;\delta u^t(z),\quad \delta u^x(z),\quad 0,\quad \delta u^z(z)\;\right). \tag{4.39}$$

The other new fields are perturbed similarly,

$$n = n_0(z) + \varepsilon e^{-i\omega t+ikx}\delta n(z)\,, \tag{4.40}$$

$$\phi = \phi_0(z) + \varepsilon e^{-i\omega t+ikx}\delta\phi(z)\,, \tag{4.41}$$

$$\rho_{fl}(n) = \rho_0(n_0(z)) + \varepsilon e^{-i\omega t+ikx}\frac{\partial\rho}{\partial n}\delta n(z) \tag{4.42}$$

$$= \rho_0(z) + \varepsilon e^{-i\omega t+ikx}\mu_0\,\delta n(z)\,. \tag{4.43}$$

The background equations of motion are changed into

$$(p_0+\rho_0)f' - 2\sqrt{f}n_0h' + 2fp' = 0\,, \tag{4.44}$$

$$4fg + fg^2(p_0+\rho_0)z^2 + gzf' + fzg' = 0\,, \tag{4.45}$$

$$-2f + 6fgz^2 + 2fgp_0z^2 + 2zf' - z^2\big(h'\big)^2 = 0\,,$$

$$-2\sqrt{f}gn_0 + z(p_0+\rho_0)gh' + 2h'' = 0\,, \tag{4.46}$$

and can no longer be solved analytically. The introduced fluid Lagrangian introduces one additional ODE to solve for the perturbations; for $\delta\phi$ inside the cloud. The obtained perturbation equations of motion are lengthy, and are included in appendix A.

This is the system considered in paper IV.

Chapter 5

Future Directions

In papers I-IV the dynamic charge response of strongly coupled matter is treated in terms bottom-up holography. Several significant properties are found, such as the strongly damped, gapped bulk plasmon in paper I, and the characteristic $\omega \propto \sqrt{k}$ dispersion of the 2D plasmon in paper II. Novel behaviour is discovered and discussed in paper III, that has not yet been accessible to experiments, and the robustness of these results through parameters space and different bulk models is observed in paper IV.

There are however several interesting questions to follow up in these papers. Firstly, these models do not take into account the lattice of positively charged ions ordinarily found in metals, which naturally introduces an additional collision-scale to the system and could have interesting effects on the theory, where initial work was begun in [54]. Secondly, many high temperature superconductors are also layered materials, where the electrons are correlated differently within layers and between layers. That is, neither the bulk nor the 2D approach presented in this may be sufficient, but rather a stack of 2D layers may be suitable, some work on this was done in [55]. Thirdly, previous work yielding holographic superconductors couple the bulk to an additional scalar field, and it would be interesting to treat those models with a proper dynamic charge response as in the paper I-IV. This is work in progress by Gran et. al.

Furthermore, as much as we can learn from bottom-up models, they inherently have a flaw in that to which extent they can be trusted is unknown. As top-down models definitely yield quantum consistent boundary theories, it would of course be of interest to have sufficiently complex top-down models that could yield the results of papers I and II, as well as incorporate the extensions proposed in the previous paragraph.

There are also numerous experimental developments targeting strange metals that would be highly beneficial for these theoretical studies, as the experimental techniques that can probe these dynamic properties of strange metals have only been available the last few years. Apart from more exper-

imental data in general, data especially near the novel behaviour found in III and IV would be of interest.

Chapter 6

Summary of papers

Paper I

Holographic plasmons

In this paper we extend the holographic framework to include long-range Coulomb interactions by deriving the necessary boundary conditions for a holographic description of plasmons and numerically perform the first holographic computation of the dispersion relation of bulk plasmons. We relate this to the known results of weakly coupled systems, as well as to different recent analytic expressions that are only valid in certain regimes. We also analyze in what parts of parameter space plasmons are the dominating relevant modes, as well as when they become similar to the previously found QNMs.

I was a significant contributor to working out the plasmon condition in terms of holographically available quantities, the key component in extending the holographic framework. I also contributed to this paper by developing the computer model as well as the numerical tools used, producing data for the different parameter setups, and graphical presentation and interpretation of the data.

Paper II

Plasmons in holographic graphene

In this paper we further extend the holographic framework and derive the necessary boundary conditions for a holographic description of all collective modes in the longitudinal and transverse sector. We elaborate on the "proper" way of introducing them, as well as the simplest possible way of doing it. We also relate the obtained dispersion relations to previously known results of weakly coupled systems, as well as different recent analytic expressions for strongly coupled systems in their limited regimes of validity.

My contribution to this paper was the generalization of the boundary

condition, to develop the computer model and the numerical tools used, producing data for the different parameter setups, graphical presentation of data and interpretation of the data.

Paper III

Exotic Holographic Dispersion

In this paper we study the bulk dispersion relations while sweeping over the parameter space. We find an exotic dispersion not exhibited by conventional weakly coupled models, in an intermediate region. This exotic region is both necessary for interpolating between known extreme parameter values as well as novel as it is only captured by higher order corrections and difficult to probe experimentally.

My contribution to this paper was the observation and highlighting of the exotic phenomena. I also performed the numerical computations, made the graphical presentations of data and provided interpretation of the data.

Paper IV

Holographic Response of Electron Clouds

In this paper we improve the model of our previous papers to also include support for a charged fermion density in the bulk. This is, to our knowledge, also the first numeric implementation of the electron "cloud" model. This introduces additional parameters of the boundary theory that can be tweaked, but the observations of our previous studies still hold, allowing us to rule out the possibility that the previously observed exotic dispersion was an artifact of the instability of the RN bulk. This inclusion also introduces an additional mode to the system.

My contribution to this paper was to develop the computer model, as well as the numerical tools used, producing data for the different parameter setups, graphical presentation of data and interpretation of the data.

Bibliography

[1] H. Kamerlingh Onnes, *Further experiments with liquid helium. d. on the change of electric resistance of pure metals at very low temperatures, etc. v. the disappearance of the resistance of mercury.*, *Comm. Phys. Lab. Univ. Leiden* **No. 122b** (1911) .

[2] J. Bardeen, L. N. Cooper and J. R. Schrieffer, *Microscopic theory of superconductivity*, *Phys. Rev.* **106** (Apr, 1957) 162–164.

[3] J. G. Bednorz and K. A. Müller, *Possible high tc superconductivity in the ba-la-cu-o system*, *Zeitschrift für Physik B Condensed Matter* **64** (Jun, 1986) 189–193.

[4] R. Zia, J. A. Schuller, A. Chandran and M. L. Brongersma, *Plasmonics: the next chip-scale technology*, *Materials Today* **9** (2006) 20 – 27.

[5] W. L. Barnes, A. Dereux and T. W. Ebbesen, *Surface plasmon subwavelength optics*, *Nature* **424** (08, 2003) 824–830.

[6] F. Nugroho, I. Darmadi, L. Cusinato, A. Susarrey Arce, H. Schreuders, L. J. Bannenberg et al., *Metal–polymer hybrid nanomaterials for plasmonic ultrafast hydrogen detection*, *Nature Materials* (05, 2019) .

[7] F. H. L. Koppens, D. E. Chang and F. J. García de Abajo, *Graphene Plasmonics: A Platform for Strong Light-Matter Interactions*, *Nano Letters* **11** (Aug., 2011) 3370–3377, [1104.2068].

[8] T. Presbyter, *Schedula diversarum artium.* ca. 1100-1120.

[9] M. I. Stockman, *Nanoplasmonics: The physics behind the applications*, *Physics Today* **62 (2), 39** (2011) .

[10] I. Langmuir, *Oscillations in ionized gases*, *Proceedings of the National Academy of Sciences* **14** (1928) 627–637, [https://www.pnas.org/content/14/8/627.full.pdf].

[11] D. Pines, *Collective energy losses in solids*, *Rev. Mod. Phys.* **28** (Jul, 1956) 184–198.

[12] S. Maier, *Plasmonics: Fundamentals and applications*. Springer US, 2007, 10.1007/0-387-37825-1.

[13] S. Szunerits and R. Boukherroub, *Introduction to Plasmonics: Advances and Applications*. Pan Stanford Publishing, 2015.

[14] D. Pines and P. Nozières, *The Theory of Quantum Liquids*. W.A. Benjamin Inc., 1966.

[15] J. D. Jackson, *From Lorenz to Coulomb and other explicit gauge transformations*, *Am. J. Phys.* **70** (2002) 917–928, [physics/0204034].

[16] B. M. Santoyo and M. del Castillo-Mussot, *Plasmons in three, two and one dimension*, *Rev. Mex. Física* **4** (1993) 640–652.

[17] M. Müller and S. Sachdev, *Collective cyclotron motion of the relativistic plasma in graphene*, *Phys. Rev.* **B78** (2008) 115419, [0801.2970].

[18] E. H. Hwang and S. Das Sarma, *Dielectric function, screening, and plasmons in two-dimensional graphene*, *Phys. Rev. B* **75** (May, 2007) 205418.

[19] B. Wunsch, T. Stauber, F. Sols and F. Guinea, *Dynamical polarization of graphene at finite doping*, *New Journal of Physics* **8** (dec, 2006) 318–318.

[20] Y. Liu and R. F. Willis, *Plasmon-phonon strongly coupled mode in epitaxial graphene*, *Phys. Rev. B* **81** (Feb, 2010) 081406.

[21] Z. Fei, G. O. Andreev, W. Bao, L. M. Zhang, A. S. McLeod, C. Wang et al., *Infrared nanoscopy of dirac plasmons at the graphene–sio2 interface*, *Nano Letters* **11** (2011) 4701–4705, [https://doi.org/10.1021/nl202362d].

[22] V. W. Brar, M. S. Jang, M. Sherrott, S. Kim, J. J. Lopez, L. B. Kim et al., *Hybrid surface-phonon-plasmon polariton modes in graphene/monolayer h-bn heterostructures*, *Nano Letters* **14** (2014) 3876–3880, [https://doi.org/10.1021/nl501096s].

[23] M. Mitrano, A. A. Husain, S. Vig, A. Kogar, M. S. Rak, S. I. Rubeck et al., *Singular density fluctuations in the strange metal phase of a copper-oxide superconductor*, 1708.01929.

[24] H. Schulz, *Fermi liquids and non-fermi liquids*, in *Proceedings of Les Houches Summer School LXI*, (Elsevier, Amsterdam), 1995.

[25] S. A. Hartnoll, J. Polchinski, E. Silverstein and D. Tong, *Towards strange metallic holography*, *JHEP* **04** (2010) 120, [0912.1061].

[26] O. Bergman, N. Jokela, G. Lifschytz and M. Lippert, *Quantum hall effect in a holographic model*, *JHEP* **1010 (063)** (2010) , [1003.4965v2].

[27] N. Jokela, G. Lifschytz and M. Lippert, *Magneto-roton excitation in a holographic quantum hall fluid*, *JHEP* **1102 (104)** (2011) , [1012.1230v3].

[28] J. Crossno, J. K. Shi, K. Wang, X. Liu, A. Harzheim, A. Lucas et al., *Observation of the Dirac fluid and the breakdown of the Wiedemann-Franz law in graphene*, *Science* **351** (Mar., 2016) 1058–1061, [1509.04713].

[29] B. Keimer, S. A Kivelson, M. R Norman, S. Uchida and J. Zaanen, *From quantum matter to high-temperature superconductivity in copper oxides*, *Nature* **518** (02, 2015) 179–86.

[30] A. Legros, S. Benhabib, W. Tabis, F. Laliberté, M. Dion, M. Lizaire et al., *Universal T-linear resistivity and Planckian dissipation in overdoped cuprates*, *Nature Physics* **15** (Nov, 2018) 142–147, [1805.02512].

[31] P. R. Wallace, *The Band Theory of Graphite*, *Phys. Rev.* **71 (622)** (1947) .

[32] S. A. Hartnoll, A. Lucas and S. Sachdev, *Holographic quantum matter*, 1612.07324.

[33] J. Zaanen, Y.-W. Sun, Y. Liu and K. Schalm, *Holographic Duality in Condensed Matter Physics*. Cambridge Univ. Press, 2015.

[34] M. Ammon and J. Erdmenger, *Gauge/gravity duality*. Cambridge University Press, 2015.

[35] J. M. Maldacena, *The Large N limit of superconformal field theories and supergravity*, *Int. J. Theor. Phys.* **38** (1999) 1113–1133, [hep-th/9711200].

[36] G. Policastro, D. T. Son and A. O. Starinets, *The Shear viscosity of strongly coupled N=4 supersymmetric Yang-Mills plasma*, *Phys. Rev. Lett.* **87** (2001) 081601, [hep-th/0104066].

[37] D. Marolf and S. F. Ross, *Boundary Conditions and New Dualities: Vector Fields in AdS/CFT*, *JHEP* **11** (2006) 085, [hep-th/0606113].

[38] I. Amado, M. Kaminski and K. Landsteiner, *Hydrodynamics of Holographic Superconductors*, *JHEP* **05** (2009) 021, [0903.2209].

[39] E. Witten, *SL(2,Z) action on three-dimensional conformal field theories with Abelian symmetry*, in *From fields to strings* (M. Shifman, A. Vainshtein and J. Wheater, eds.), vol. 2, pp. 1173–1200. World Scientific, 2003. hep-th/0307041.

[40] E. Witten, *Multitrace operators, boundary conditions, and AdS / CFT correspondence*, hep-th/0112258.

[41] W. Mueck, *An Improved correspondence formula for AdS / CFT with multitrace operators*, *Phys. Lett.* **B531** (2002) 301–304, [hep-th/0201100].

[42] M. Edalati, J. I. Jottar and R. G. Leigh, *Holography and the sound of criticality*, *JHEP* **10** (2010) 058, [1005.4075].

[43] R. A. Davison and N. K. Kaplis, *Bosonic excitations of the AdS_4 Reissner-Nordstrom black hole*, *JHEP* **12** (2011) 037, [1111.0660].

[44] D. Forcella, A. Mezzalira and D. Musso, *Electromagnetic response of strongly coupled plasmas*, *JHEP* **11** (2014) 153, [1404.4048].

[45] A. Amariti, D. Forcella, A. Mariotti and G. Policastro, *Holographic Optics and Negative Refractive Index*, *JHEP* **04** (2011) 036, [1006.5714].

[46] L. Liu and H. Liu, *Wake potential in a strong coupling plasma from the AdS/CFT correspondence*, *Phys. Rev.* **D93** (2016) 085011, [1502.01841].

[47] G. Mahan, *Many-Particle Physics*. Physics of Solids and Liquids. Springer US, 2000.

[48] J. Lucietti, K. Murata, H. S. Reall and N. Tanahashi, *On the horizon instability of an extreme Reissner-Nordström black hole*, *JHEP* **03** (2013) 035, [1212.2557].

[49] S. Aretakis, *Stability and Instability of Extreme Reissner-Nordström Black Hole Spacetimes for Linear Scalar Perturbations I*, *Commun. Math. Phys.* **307** (2011) 17–63, [1110.2007].

[50] S. Aretakis, *Stability and Instability of Extreme Reissner-Nordstrom Black Hole Spacetimes for Linear Scalar Perturbations II*, *Annales Henri Poincare* **12** (2011) 1491–1538, [1110.2009].

[51] S. A. Hartnoll, C. P. Herzog and G. T. Horowitz, *Building a Holographic Superconductor*, *Phys. Rev. Lett.* **101** (2008) 031601, [0803.3295].

[52] S. A. Hartnoll, C. P. Herzog and G. T. Horowitz, *Holographic Superconductors*, *JHEP* **12** (2008) 015, [0810.1563].

[53] R. Amorim, *Charged spinning fluids in general relativity*, *Physics Letters A* **104** (1984) 259 – 261.

[54] M. Baggioli, U. Gran, A. J. Alba, M. Tornsö and T. Zingg, *Holographic Plasmon Relaxation with and without Broken Translations*, 1905.00804.

[55] E. Mauri and H. T. C. Stoof, *Screening of Coulomb interactions in Holography*, *JHEP* **04** (2019) 035, [1811.11795].

Appendix A

Perturbation equations

These are the equations of motion for the electron cloud bulk model. The equations of motion for the Reissner-Nordström bulk model are similar, and obtained by letting $\sigma \to 0$.

A.1 Equations of motion

δA_t-variation equation:

$$\begin{aligned}
&\delta A_t'' - k^2 \delta A_t g z^2 + \frac{k \delta g_{tx} f^{1/2} g \sigma z^2}{\omega} + \frac{i k^2 \delta\phi f^{3/2} g \sigma z^2}{\omega h} \\
&+ \frac{\delta A_x \left(-k\omega^2 g h z^2 + k f^{3/2} g \sigma z^2\right)}{\omega h} + \frac{\delta A_t' \left(-4fg - gzf' - fzg'\right)}{2fgz} + \frac{\delta g_{tt}' h'}{2f} \\
&+ \tfrac{1}{2} z^2 \delta g_{xx}' h' + \tfrac{1}{2} z^2 \delta g_{yy}' h' + \tfrac{1}{2} \delta g_{xx} \left(f^{1/2} g \sigma z^2 + 2 z h'\right) + \tfrac{1}{2} \delta g_{yy} \left(f^{1/2} g \sigma z^2 + 2 z h'\right) \\
&- \frac{i f^{1/2} \delta\phi' \left(-4 f g h \sigma + 2 g h \sigma z f' - f h \sigma z g' - 2 f g \sigma z h' + 2 f g h z \sigma'\right)}{2\omega g h^2 z} \\
&- \frac{i f^{3/2} \sigma \delta\phi''}{\omega h} + \frac{\delta g_{tt} \left(-f^{3/2} g^2 \sigma z - 4 f g h' - 2 g z f' h' - f z g' h' + 2 f g z h''\right)}{2 f^2 g z} = 0
\end{aligned}$$

δA_x-variation equation:

$$\begin{aligned}
&\frac{k\omega \delta A_t g}{f} - \frac{i k \delta\phi f^{1/2} g \sigma}{h} + \frac{\delta A_x g \left(\omega^2 h - f^{3/2} \sigma\right)}{f h} + \frac{\delta A_x' \left(g f' - f g'\right)}{2 f g} + \frac{\delta g_{tx}' h'}{f} \\
&+ \delta A_x'' + \frac{\delta g_{tx} \left(-2 f^{3/2} g^2 \sigma - g f' h' - f g' h' + 2 f g h''\right)}{2 f^2 g} = 0
\end{aligned}$$

$\delta\phi$-equation, from n-variation:

$$\delta\phi'' + ik\delta A_x g z^2 + \frac{ik\delta g_{tx} g h z^2}{f} + \frac{i\omega\delta g_{xx} g h z^2}{2f} + \frac{i\omega\delta g_{yy} g h z^2}{2f} + \frac{i\omega\delta A_t g h\sigma'}{f^{3/2}\sigma\mu'}$$
$$+ \frac{i\omega\delta g_{tt} g h^2\sigma'}{2f^{5/2}\sigma\mu'} - \tfrac{1}{2}\delta\phi'\big(\frac{4}{z} - \frac{2f'}{f} + \frac{g'}{g} + \frac{2h'}{h} - \frac{2\sigma'}{\sigma}\big) - \delta\phi g\Big(k^2 z^2 - \frac{\omega^2 h\sigma'}{f^{3/2}\sigma\mu'}\Big) = 0$$

δg_{tt}-variation equation:

$$\delta g_{tt}'' + 2f^{1/2} g\sigma\delta A_t - \frac{k f^{3/2} g\sigma z^2}{\omega}\delta A_x - \frac{kg\Big(\omega^2 + f^{1/2} h\sigma\Big)z^2}{\omega}\delta g_{tx}$$
$$- \frac{i\Big(2\omega^2 f^{1/2} g\sigma + k^2 f^{3/2} g\sigma z^2\Big)}{\omega}\delta\phi + \tfrac{1}{4}\big(-2fz - z^2 f'\big)\delta g_{xx}'$$
$$+ \tfrac{1}{4}\big(-2fz - z^2 f'\big)\delta g_{yy}' + \frac{\big(-2fg - 2gzf' - fzg'\big)}{2fgz}\delta g_{tt}' + 3h'\delta A_t'$$
$$+ \frac{if^{1/2}\big(-4fgh\sigma + 2gh\sigma zf' - fh\sigma zg' - 2fg\sigma zh' + 2fghz\sigma'\big)}{2\omega ghz}\delta\phi'$$
$$+ \frac{if^{3/2}\sigma}{\omega}\delta\phi''$$
$$+ \frac{1}{2f^2 gz^2}\Big(10f^2 g - 6f^2 g^2 z^2 + 2f^2 g^2\rho z^2 + 2f^{3/2} g^2 h\sigma z^2 - k^2 f^2 g^2 z^4 + 2fgzf'$$
$$+2gz^2\big(f'\big)^2 + 2f^2 zg' + fz^2 f'g' + 4fgz^2\big(h'\big)^2 - 2fgz^2 f''\Big)\delta g_{tt}$$
$$+ \frac{1}{4fg}\Big(4f^2 g - 2\omega^2 fg^2 z^2 - 12f^2 g^2 z^2 + 4f^2 g^2\rho z^2 - 6f^{3/2} g^2 h\sigma z^2 - 4fgzf'$$
$$-gz^2\big(f'\big)^2 + 2f^2 zg' - fz^2 f'g' - 2fgz^2\big(h'\big)^2 + 2fgz^2 f''\Big)\delta g_{xx}$$
$$+ \frac{1}{4fg}\Big(4f^2 g - 2\omega^2 fg^2 z^2 - 12f^2 g^2 z^2 + 4f^2 g^2\rho z^2 - 6f^{3/2} g^2 h\sigma z^2 - 2k^2 f^2 g^2 z^4$$
$$-4fgzf' - gz^2\big(f'\big)^2 + 2f^2 zg' - fz^2 f'g' - 2fgz^2\big(h'\big)^2 + 2fgz^2 f''\Big)\delta g_{yy}$$
$$= 0$$

δg_{tx}-variation equation:

$$\delta g_{tx}'' + 2\delta A_x f^{1/2} g\sigma + 2ik\delta\phi f^{1/2} g\sigma + k\omega\delta g_{yy} g z^2 + \frac{\delta g_{tx}'\big(-gf' - fg'\big)}{2fg}$$
$$+ 2\delta A_x' h' + \delta g_{tx}\Big(-6g + 2g\rho + \frac{4}{z^2} - \frac{f'}{fz} + \frac{g'}{gz} + \frac{\big(h'\big)^2}{f}\Big) = 0$$

δg_{yy}-variation equation:

$$\begin{aligned}
&\delta g''_{yy} - \frac{k\delta A_x f^{1/2} g\sigma}{\omega} - \frac{ik^2\delta\phi f^{1/2} g\sigma}{\omega} - \frac{k\delta g_{tx} g\left(\omega^2 + f^{1/2}h\sigma\right)}{\omega f} \\
&+ \frac{\delta g'_{xx}\left(-2f - zf'\right)}{4fz} + \frac{\delta g'_{yy}\left(6fg + gzf' - 2fzg'\right)}{4fgz} + \frac{\delta A'_t h'}{fz^2} \\
&+ \frac{\delta g_{tt}\left(10fg - 6fg^2z^2 + 2fg^2\rho z^2 - k^2 fg^2 z^4 + 2fzg' + 2gz^2\left(h'\right)^2\right)}{2f^2 g z^4} \\
&+ \frac{i\delta\phi'\left(-4fgh\sigma + 2gh\sigma zf' - fh\sigma zg' - 2fg\sigma zh' + 2fgh z\sigma'\right)}{2\omega f^{1/2} g h z^3} + \frac{if^{1/2}\sigma\delta\phi''}{\omega z^2} \\
&+ \frac{1}{4f^2 g z^2}\Big(-12f^2 g - 2\omega^2 fg^2 z^2 + 12f^2 g^2 z^2 - 4f^2 g^2\rho z^2 + 2f^{3/2} g^2 h\sigma z^2 \\
&\qquad + gz^2\left(f'\right)^2 - 2f^2 zg' + fz^2 f'g' + 2fgz^2\left(h'\right)^2 - 2fgz^2 f''\Big)\delta g_{xx} \\
&+ \frac{1}{4f^2 g z^2}\Big(-4f^2 g + 2\omega^2 fg^2 z^2 - 12f^2 g^2 z^2 + 4f^2 g^2\rho z^2 - 6f^{3/2} g^2 h\sigma z^2 \\
&-2k^2 f^2 g^2 z^4 - gz^2\left(f'\right)^2 - 2f^2 zg' - fz^2 f'g' - 2fgz^2\left(h'\right)^2 + 2fgz^2 f''\Big)\delta g_{yy} \\
&\qquad = 0
\end{aligned}$$

δg_{xx}-variation equation:

$$\begin{aligned}
&+ \delta g''_{xx} - \frac{k\delta A_x f^{1/2} g\sigma}{\omega} - \frac{ik^2\delta\phi f^{1/2} g\sigma}{\omega} + \frac{k\delta g_{tx} g\left(\omega^2 - f^{1/2}h\sigma\right)}{\omega f} \\
&+ \frac{\delta g'_{yy}\left(-2f - zf'\right)}{4fz} + \frac{\delta g'_{xx}\left(6fg + gzf' - 2fzg'\right)}{4fgz} + \frac{\delta A'_t h'}{fz^2} \\
&+ \frac{\delta g_{tt}\left(10fg - 6fg^2z^2 + 2fg^2\rho z^2 + k^2 fg^2 z^4 + 2fzg' + 2gz^2\left(h'\right)^2\right)}{2f^2 g z^4} \\
&+ \frac{i\delta\phi'\left(-4fgh\sigma + 2gh\sigma zf' - fh\sigma zg' - 2fg\sigma zh' + 2fgh z\sigma'\right)}{2\omega f^{1/2} g h z^3} \\
&+ \frac{if^{1/2}\sigma\delta\phi''}{\omega z^2} \\
&+ \frac{1}{4f^2 g z^2}\Big(-12f^2 g - 2\omega^2 fg^2 z^2 + 12f^2 g^2 z^2 - 4f^2 g^2\rho z^2 + 2f^{3/2} g^2 h\sigma z^2 \\
&-2k^2 f^2 g^2 z^4 + gz^2\left(f'\right)^2 - 2f^2 zg' + fz^2 f'g' + 2fgz^2\left(h'\right)^2 - 2fgz^2 f''\Big)\delta g_{yy} \\
&+ \frac{1}{4f^2 g z^2}\Big(-4f^2 g + 2\omega^2 fg^2 z^2 - 12f^2 g^2 z^2 + 4f^2 g^2\rho z^2 - 6f^{3/2} g^2 h\sigma z^2 \\
&\qquad - gz^2\left(f'\right)^2 - 2f^2 zg' - fz^2 f'g' - 2fgz^2\left(h'\right)^2 + 2fgz^2 f''\Big)\delta g_{xx} \\
&\qquad = 0
\end{aligned}$$

A.2 Constraint equations

δg_{tz}-variation, constraint equation:

$$\frac{ikz^2\delta g'_{tx}}{2fg}+\frac{i\omega z^2\delta g'_{xx}}{2fg}+\frac{i\omega z^2\delta g'_{yy}}{2fg}-\frac{\sigma\delta\phi'}{f^{1/2}g}-\frac{ik\delta g_{tx}z^2f'}{2f^2g}+\frac{i\omega\delta g_{xx}z\big(2f-zf'\big)}{4f^2g}+\frac{i\omega\delta g_{yy}z\big(2f-zf'\big)}{4f^2g}=0$$

δg_{xz}-variation, constraint equation:

$$-\frac{i\omega\delta g_{tx}z}{fg}+\frac{ik\delta g_{yy}z^3}{g}-\frac{ikz^2\delta g'_{tt}}{2fg}-\frac{i\omega z^2\delta g'_{tx}}{2fg}+\frac{ikz^4\delta g'_{yy}}{2g}+\frac{i\delta g_{tt}z\big(-2kf+kzf'\big)}{4f^2g}-\frac{ik\delta A_tz^2h'}{fg}-\frac{i\omega\delta A_xz^2h'}{fg}=0$$

δg_{zz}-variation, constraint equation:

$$\frac{\delta A_t\sigma}{f^{1/2}g}-\frac{i\omega\delta\phi\sigma}{f^{1/2}g}-\frac{k\omega\delta g_{tx}z^2}{fg}-\frac{\delta g'_{tt}}{fg^2z}+\frac{z\delta g'_{xx}\big(2f-zf'\big)}{4fg^2}+\frac{z\delta g'_{yy}\big(2f-zf'\big)}{4fg^2}+\frac{\delta g_{xx}\Big(2f-z\big(\omega^2gz+f'\big)\Big)}{2fg^2}+\frac{\delta g_{yy}\Big(f\big(2+k^2gz^4\big)-z\big(\omega^2gz+f'\big)\Big)}{2fg^2}-\frac{\delta A'_th'}{fg^2}+\frac{\delta g_{tt}\Big(f^{1/2}gh\sigma z-k^2fgz^3+2f'-z\big(h'\big)^2\Big)}{2f^2g^2z}=0$$

δA_z-variation, constraint equation:

$$\frac{i\omega\delta A'_t}{fg}+\frac{ikz^2\delta A'_x}{g}+\frac{f^{1/2}\sigma\delta\phi'}{gh}+\frac{i\omega\delta g_{tt}h'}{2f^2g}+\frac{ik\delta g_{tx}z^2h'}{fg}+\frac{i\omega\delta g_{xx}z^2h'}{2fg}+\frac{i\omega\delta g_{yy}z^2h'}{2fg}=0$$